Journal of Pharmaceutical Analysis 12 (2022) 453–459

Contents lists available at ScienceDirect

Journal of Pharmaceutical Analysis

journal homepage: www.elsevier.com/locate/jpa

Original article

Highly sensitive electrochemical determination of rutin based on the synergistic effect of 3D porous carbon and cobalt tungstate nanosheets

Guangjun Feng [a, 1], Yang Yang [a, 1], Jiantao Zeng [c], Jun Zhu [b], Jingjian Liu [b], Lun Wu [b], Zhiming Yang [a], Guanyi Yang [a], Quanxi Mei [a], Qinhua Chen [a, *], Fengying Ran [b, **]

[a] Shenzhen Baoan Authentic TCM Therapy Hospital, Shenzhen, 518101, China
[b] Sinopharm Dongfeng General Hospital, Hubei University of Medicine, Shiyan, Hubei, 442008, China
[c] Shenzhen Hospital of Integrated Traditional Chinese and Western Medicine, Shenzhen, 518101, China

ARTICLE INFO

Article history:
Received 6 March 2021
Received in revised form
7 September 2021
Accepted 15 September 2021
Available online 16 September 2021

Keywords:
Rutin
Electrochemical detection
$CoWO_4$ nanosheets
Porous carbon
Sensor

ABSTRACT

Rutin, a flavonoid found in fruits and vegetables, is a potential anticancer compound with strong anticancer activity. Therefore, electrochemical sensor was developed for the detection of rutin. In this study, $CoWO_4$ nanosheets were synthesized via a hydrothermal method, and porous carbon (PC) was prepared via high-temperature pyrolysis. Successful preparation of the materials was confirmed, and characterization was performed by transmission electron microscopy, scanning electron microscopy, and X-ray photoelectron spectroscopy. A mixture of PC and $CoWO_4$ nanosheets was used as an electrode modifier to fabricate the electrochemical sensor for the electrochemical determination of rutin. The 3D $CoWO_4$ nanosheets exhibited high electrocatalytic activity and good stability. PC has a high surface-to-volume ratio and superior conductivity. Moreover, the hydrophobicity of PC allows large amounts of rutin to be adsorbed, thereby increasing the concentration of rutin at the electrode surface. Owing to the synergistic effect of the 3D $CoWO_4$ nanosheets and PC, the developed electrochemical sensor was employed to quantitively determine rutin with high stability and sensitivity. The sensor showed a good linear range (5–5000 ng/mL) with a detection limit of 0.45 ng/mL. The developed sensor was successfully applied to the determination of rutin in crushed tablets and human serum samples.

1. Introduction

Traditional Chinese medicine plays an irreplaceable role in the Chinese healthcare system [1]. Flavonoids, which are found in many types of plants, are commonly used in traditional Chinese medicine. In addition to their important role in the growth and development of plants, these compounds have antibacterial, antiviral, antitumor, anti-inflammatory, anti-cancer, and anti-aging properties and can be used to treat cardiovascular and cerebrovascular diseases [2,3]. Rutin (vitamin P; Fig. 1) is a common flavonoid glycoside present in many types of plants [4], and its physiological functions (including anti-tumor, anti-inflammatory, anti-bacterial, anti-aging, anti-oxidant, anti-hemorrhagic, and anti-myocardial hypoxia) have been confirmed by many studies [5,6]. Thus, in recent decades, rutin has been used for clinical applications because of its remarkable physiological activity and medicinal value. Therefore, it is of great significance to establish highly sensitive and stable analytical methods for rutin determination.

Various analytical sensors have been developed for rutin determination, for instance, chemiluminescence [7], fluorescence [8], spectrophotometry [9], high-performance liquid chromatography [10], capillary electrophoresis [11,12], and voltammetry [13].

Peer review under responsibility of Xi'an Jiaotong University.
* Corresponding author.
** Corresponding author.
E-mail addresses: cqh77@163.com (Q. Chen), ranfengying13@163.com (F. Ran).
[1] Both authors contributed equally to this work.

https://doi.org/10.1016/j.jpha.2021.09.007

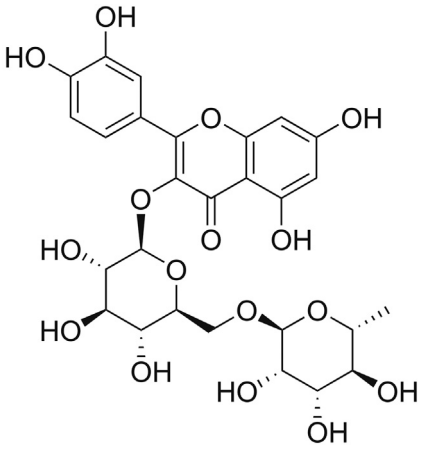

Fig. 1. Molecular structures of rutin.

These sensors have the advantages of high accuracy and sensitivity, but they are expensive, time-consuming, and are often complicated to operate, thus limiting their application. Electrochemical detection is also commonly employed [14–16] and has the advantages of rapid reaction time, fast analysis, a low detection limit, and high sensitivity [17–19]. Moreover, the electrode can be modified with various materials to improve its performance. Many of the developed electrochemical methods, however, require acidic conditions for rutin detection. Because rutin is easily oxidized under acidic conditions and its oxidation current is weak under physiological conditions, it is imperative to develop a highly sensitive electrochemical sensor that detects rutin under physiological (i.e., non-acidic) conditions.

In recent years, various nanomaterials with good conductivity and excellent electrocatalytic activity have been developed for use as electrode modifiers for electrochemical sensors. Transition metal oxides [20] such as Co_3O_4 have shown significant potential as electrode materials for electrochemical biosensors because of their low cost, natural abundance, and rich redox chemistry. However, their relatively poor cycle stability and low electrical conductivity limit its potential as an electrode modifier for electrochemical sensors [21]. The introduction of tungsten (W) element significantly enhanced the electrical conductivity [22], and $CoWO_4$ exhibits superior electrocatalytic activity compared to Co_3O_4 due to the ability of W to occupy multiple valence states. The morphology of $CoWO_4$ is found to have a vital effect on its electrochemical performance [22]. Recently, two-dimensional (2D) nanomaterials have attracted wide interest in the field of electrochemical sensors owing to their excellent electrochemical performance [23,24]. This is because they have a large surface-to-volume ratio, increasing the number of active sites and offering a larger area for the adsorption of target molecules [25,26]. However, it should be noted that 2D nanosheets tend to aggregate as a result of their high surface energies and the strong van der Waals attractive forces between the nanosheets [27]. However, using 2D nanomaterials as basic components to assemble three-dimensional (3D) architectures not only prevents the aggregation problem but also exposes more electrocatalytic active sites owing to the increased porosity, exhibits better cycling stability, and has a larger specific surface area [28,29]. $CoWO_4$, a p-type semiconductor with a relatively low conductivity, requires a conducting support material to be used as an electrode modifier. Porous carbon (PC), produced via the pyrolysis of potassium citrate at 800 °C, has a high conductivity, high porosity, and is relatively chep to produce [30]. Its high surface-volume ratio and good conductivity facilitate the adsorption of more substances for detection with successful transfer of electrons. Therefore, the high surface-volume ratio and hydrophobicity of PC are beneficial for the absorption of rutin. The electrochemical signal for rutin adsorption is predominantly a function of its concentration at the electrode surface. Therefore, the introduction of PC as a conducting support can significantly improve the electrochemical performance of 3D $CoWO_4$ for sensing rutin.

In this work, $CoWO_4$ nanosheets were first prepared via a one-step hydrothermal technique. The obtained $CoWO_4$ nanosheets exhibited a 3D structure consisting of numerous 2D nanosheets. The 3D $CoWO_4$ exhibited a large surface-volume ratio, high porosity, and good stability. The 3D $CoWO_4$ was mixed with PC via the pyrolysis of potassium citrate at 800 °C, and the resultant mixture was used to fabricate the electrochemical sensor. The performance of the proposed sensor was investigated under optimal conditions. The developed electrochemical sensor exhibited ultra-high sensitivity, good stability, and reproducibility, and was successfully applied for the determination of rutin in tablets and human serum samples.

2. Experimental

2.1. Materials

$Na_2WO_4 \cdot 2H_2O$, $CoCl_2 \cdot 6H_2O$, and potassium citrate were purchased from Aladdin Reagent Co., Ltd. (Shanghai, China). Rutin was obtained from Chengdu Herbpurify Co., Ltd. (Chengdu, China). Biological samples (i.e., healthy human serum samples) were obtained from Sinopharm Dongfeng General Hospital (Shiyan, China) and approved by the Sinopharm Dongfeng General Hospital Ethics Committee. All other reagents were of analytical grade. Ultrapure water (18.2 MΩ cm; Milli-Q Direct 8, Millipore, Shanghai, China) was used in all runs and was prepared using a Millipore direct water-purification system.

2.2. Preparation of $CoWO_4$ and PC

$CoWO_4$ nanosheets were synthesized as follows (Fig. 2). $Na_2WO_4 \cdot 2H_2O$ (0.033 g) and $CoCl_2 \cdot 6H_2O$ (0.02 g) were homogeneously mixed in distilled water (DW; 50 mL) using a magnetic stirrer and ultrasound mixing. Obtained solution was poured into 100 mL Teflon-lined stainless-steel autoclaves (Anhui Kemi Machinery Technology Co., Ltd., Hefei, China) and sealed at 200 °C for 10 h at a heating rate of 5 °C/min. The products were collected after cooling to room temperature and washed with ethanol and DW before drying for 6 h at 90 °C.

PC was synthesized as described by Wan and co-workers et al. [30]: potassium citrate (8 mmol; Alpha Aesar Co., Ltd., Shanghai, China) was added to a tube furnace and pyrolyzed for 1 h at 800 °C under Ar atmosphere. The obtained black solid product was washed with water and H_2SO_4 solution (0.5 mM; Alpha Aesar Co., Ltd., Shanghai, China) until the solution was neutral and then freeze-dried to obtain PC.

2.3. Preparation of electrodes and electrochemical measurements

The glassy carbon electrode (Φ = 3 mm) was polished with 0.3 μm and 0.05 μm γ-alumina powders (CH Instruments, Shanghai, China), and any residual alumina powder was removed via ultrasonic treatment with water and ethanol for 5 min. After electrochemical cleaning with H_2SO_4 (0.5 M), the glassy carbon electrode was cleaned with ultrapure water, and the prepared electrode was dried with nitrogen. $CoWO_4$ powder (1 mg) and PC (1 mg) were dispersed in a water/ethanol/Nafion mixture

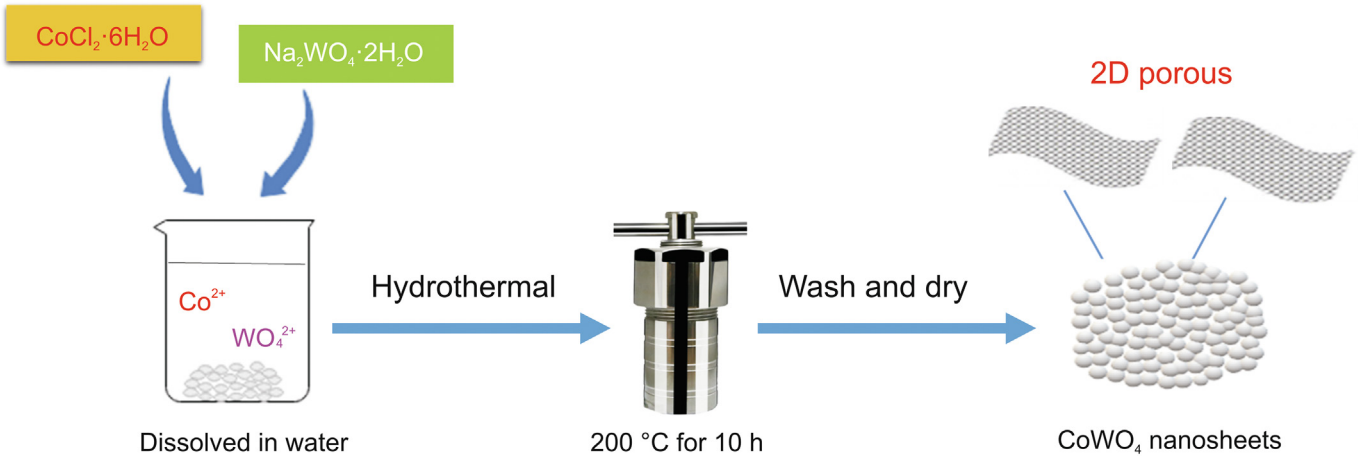

Fig. 2. Illustration of the synthetic procedures for $CoWO_4$ nanosheets.

(95:95:10, *V*/*V*/*V*; 2 mL) under sonication for 30 min. The prepared dispersion solution (10 μL) was dripped onto the surface of the pretreated electrodes before drying in air.

In this work, a conventional three-electrode system was used for all electrochemical experiments, and all electrochemical measurements were performed on a CHI 660D electrochemical workstation (CH Instruments, Shanghai, China). The modified glassy carbon electrode acted as the working electrode while a saturated calomel electrode and a platinum electrode served as the reference electrode and auxiliary electrodes, respectively (Gaoss Union, Wuhan, China). Differential pulse voltammetry (DPV) measurements were carried out in a rutin-containing phosphate-buffered saline (PBS) solution by scanning the potential range from −0.2 V to 0.6 V with an amplitude of 0.05 V, a frequency of 25 Hz, and a step potential of 4 mV. Electrochemical impedance spectroscopy (EIS) was performed in a PBS solution (0.01 M) containing KCl (0.1 M) and $[Fe(CN)_6]^{3-/4-}$ (5 mM) at frequencies ranging from 1 Hz to 100 kHz and with an amplitude of 5 mV.

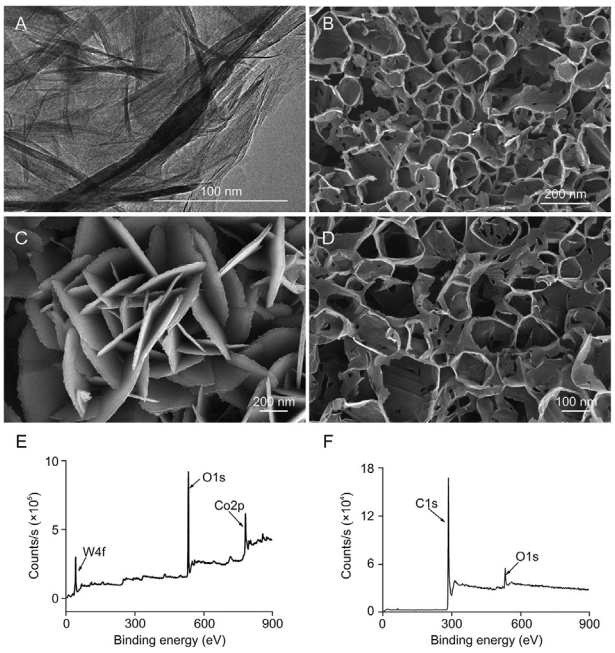

Fig. 3. Transmission electron microscopy images of (A) $CoWO_4$ and (B) Porous carbon (PC), scanning electron microscopy images of (C) $CoWO_4$ and (D) PC nanosheets, and X-ray photoelectric spectroscopy patterns of (E) $CoWO_4$ and (F) PC.

3. Results and discussion

3.1. Characterization of $CoWO_4$ and PC

The morphologies of $CoWO_4$ and PC (Fig. 3) were investigated by transmission electron microscopy (TEM), scanning electron microscopy (SEM), and X-ray photoelectron spectroscopy (XPS). As shown in Fig. 3A, TEM analysis revealed that $CoWO_4$ adopted a nanobelt structure. SEM analysis revealed that the synthesized $CoWO_4$ had a 3D structure and was composed of numerous nanosheets (Fig. 3C). This 3D structure increases the number of exposed catalytic active sites, thus improving the catalytic utilization efficiency of $CoWO_4$. We can also estimate the thickness and height of the $CoWO_4$ nanosheet material to be approximately 10 and 1000 nm, respectively, from the SEM image. Elemental peaks were determined in the XPS spectrum of $CoWO_4$ (Fig. 3E). PC was found to have a dense porous nanostructure (Figs. 3B and D). The average aperture size was approximately 200 nm, which is similar to that reported in the literature [31]. This dense nanopore structure not

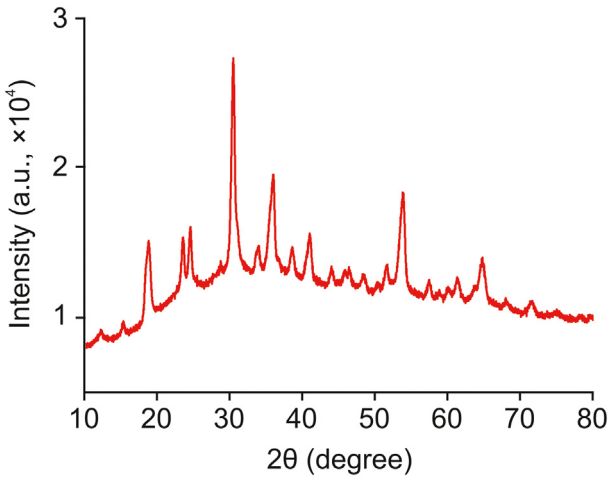

Fig. 4. X-ray diffraction patterns of $CoWO_4$ nanocomposites.

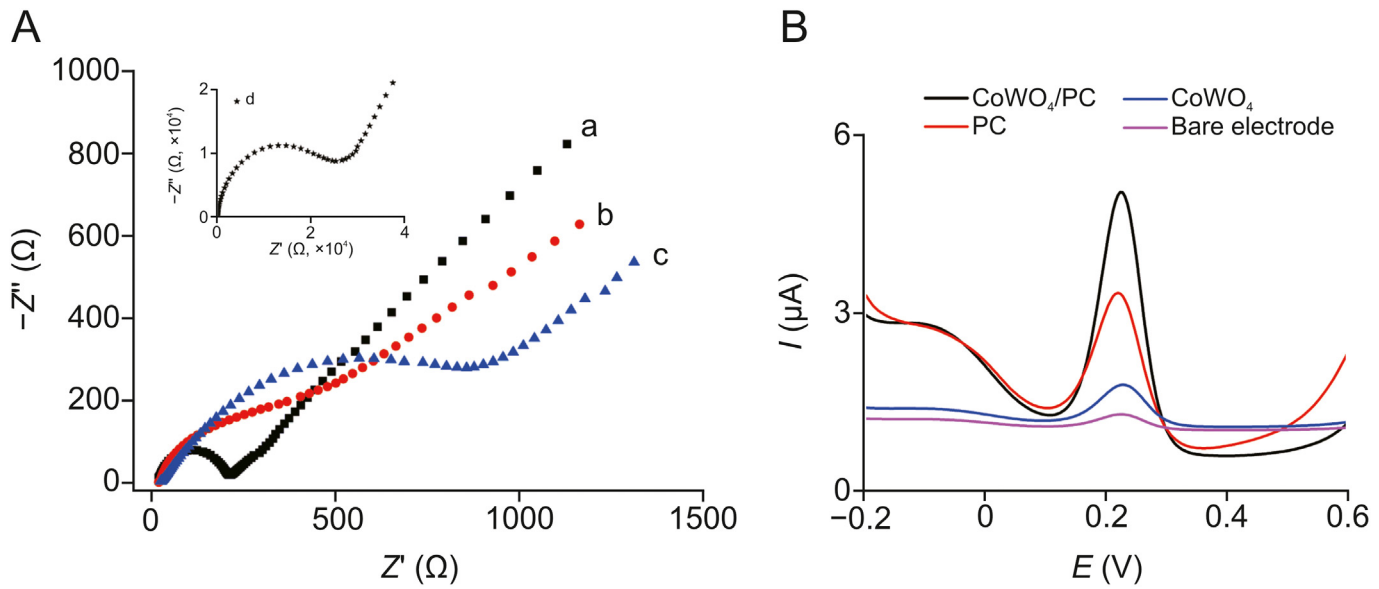

Fig. 5. (A) Electrochemical impedance spectroscopy of different modified electrodes in solution containing 0.1 M KCl and 5 mM $[Fe(CN)_6]^{3-/4-}$. (B) Differential pulse voltammetry (DPV) of different modified electrodes after enrichment for the same time in phosphate-buffered saline (PBS) solution containing 50 ng/mL rutin. (a) Bare gold electrode (230 Ω, 0.12); (b) PC-modified electrode (400 Ω, 2.02); (c) PC/$CoWO_4$ -modified electrode (880 Ω, 4.03); and (d) $CoWO_4$ -modified electrode (26,000 Ω, 1.32).

only facilitates electron transport but also facilitates the adsorption of more rutin. Fig. 3F shows the XPS profile of PC, which is consistent with that in the literature reports [31]. These results further confirmed the successful synthesis of $CoWO_4$ nanosheets. X-ray diffraction patterns were obtained for the $CoWO_4$ nanocomposites (Fig. 4), and only the characteristic peaks of the $CoWO_4$ nanosheets were observed. $CoWO_4$ structure is similar to that reported in the literature [32]. The narrow and strong diffraction peaks indicate a high degree of crystallinity in the nanosheets. This analysis confirmed the successful synthesis of $CoWO_4$ and PC.

3.2. Electrochemical characterization

The construction process of the electrochemical sensor was characterized via EIS and DPV. Fig. 5 shows the EIS and DPV results for the gold electrode at different construction stages to illustrate the magnitude of the resistance and the electrode performance, respectively. The EIS consists of a linear part and a semicircular part which reveal information about the modification process of the sensors, while the semicircular diameter represents the charge transfer resistance (Ret)-limited process [33,34]. As shown in Fig. 5A, the Ret of the PC-modified electrodes (Fig. 5A, curve b; approximately 400 Ω) was slightly larger than that of the bare electrode (Fig. 5A, curve a; approximately 230 Ω), indicating good electrical conductivity in the PC-modified electrode. However, when the electrode was modified with $CoWO_4$, the Ret was very large (Fig. 5A, insert curve d; approximately 26,000 Ω), and this was attributed to its poor electrical conductivity. However, the Ret of the PC/$CoWO_4$-modified electrode decreased to approximately 880 Ω (Fig. 5A, curve c), confirming that the addition of PC improved the electrical conductivity of $CoWO_4$.

The electrochemical behavior of these modified electrodes in the determination of rutin was explored by DPV. As shown in Fig. 5B, the redox peak currents (I_p) of the bare electrode are negligible. This is mainly attributed to two reasons: 1) the catalytic activity of the bare electrode for rutin was very low, and 2) the adsorption of rutin on the bare electrode surface is negligible. The I_p of the $CoWO_4$-modified electrode was slightly higher than that of the bare electrode. $CoWO_4$ has good electrocatalytic activity for rutin, but its poor electrical conductivity limits its detection performance. The I_p of the PC-modified electrode was significantly higher than that of the bare electrode. This is attributed to the good electrical conductivity of PC, which allowed for large amounts of rutin to be adsorbed on the electrode surface. The I_p of the PC/$CoWO_4$-modified electrode was nearly twice that of the PC-modified electrode. The excellent performance of this PC/$CoWO_4$-modified electrode is attributed to the synergistic effect of the excellent conductivity and enrichment capacity of PC and the excellent catalytic activity of $CoWO_4$.

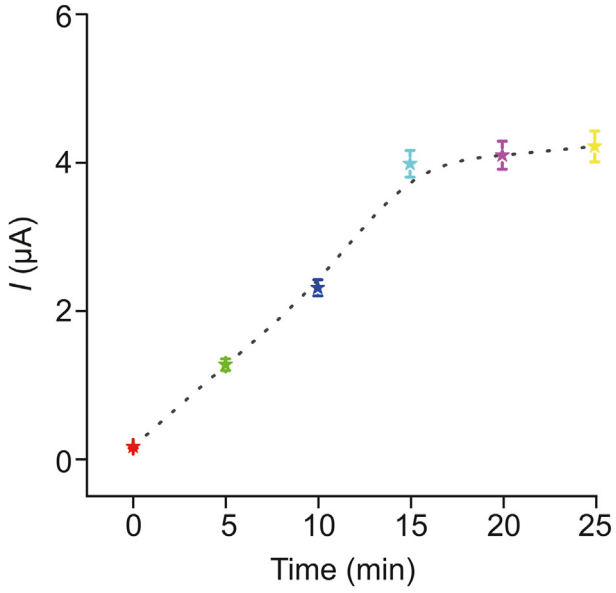

Fig. 6. Effect of the enrichment time on the electrochemical sensing of rutin. Error bars: standard deviation ($n = 3$).

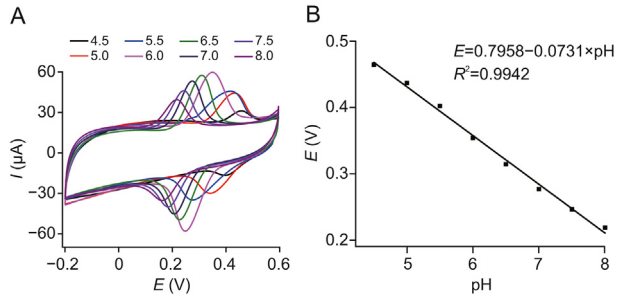

Fig. 7. (A) DPVs of rutin (50 ng/mL) samples in PBS solution with varying pH values (from left to right: pH = 8.0, 7.5, 7.0, 6.5, 6.0, 5.5, 5.0, and 4.5). (B) Effect of pH on the anodic peak potentials of rutin samples (50 ng/mL). Error bars: standard deviation ($n = 3$).

3.3. Optimization of conditions for biosensing

The electrochemical signal of the detected substance is mainly based on its concentration at the electrode surface [35,36]. As mentioned above, PC was found to have a dense nanoporous structure and good hydrophobicity, both of which are beneficial for the adsorption of rutin. Enrichment time had a significant effect on the current signal. As can be seen from Fig. 6, when the enrichment time was less than 15 min, the current increased with increasing enrichment time. When the enrichment time increased to 20 min, the change in the current response value can be ignored as it reached a relatively stable state. Therefore, 15 min was set as the optimal enrichment time for the following experiments.

The effect of pH on the electrochemical performance was studied to investigate the performance of the fabricated electrochemical sensor platform. As shown in Fig. 7A, the acidity of the buffer solution had a significant effect on the electrochemical detection of rutin. The effect of pH values (ranging from 4.5 to 8.0) on the electrochemical response was studied by DPV. It was found that the redox peak changed under different pH conditions: when the pH decreased from 8 to 4.5, the peak current first increased and then decreased. The impact of pH on the peak current is a result of several factors. The oxidation peak current of rutin was found to be different at different pH values. The catalytic activity of $CoWO_4$ was also found to change with pH. Furthermore, the enrichment efficiency of PC for

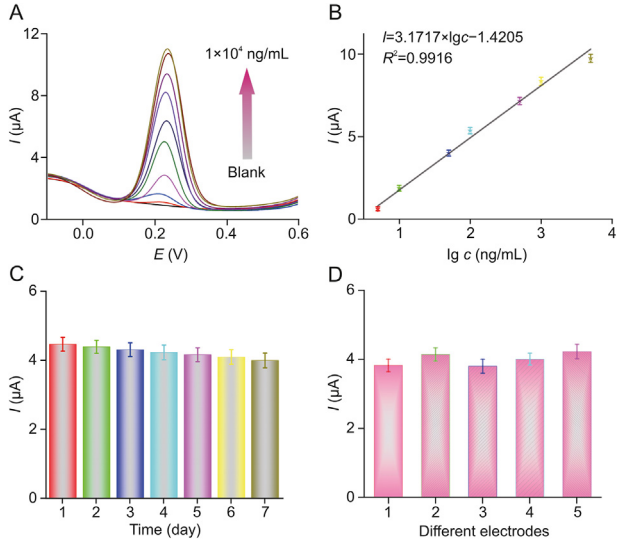

Fig. 8. (A) DPV curves of different concentrations of rutin in buffer (from bottom to top: 0, 1, 5, 10, 50, 100, 500, 1000, 5000, and 10,000 ng/mL). (B) Linear relationships between DPV current and lg of rutin concentration ranging from 5 to 5000 ng/mL, $I = 3.1717 \times \lg c - 1.4205$ ($R^2 = 0.9916$). (C) Stability and (D) reproducibility of the electrochemical sensor. The numbers 1 to 5 indicate five bare glassy carbon electrodes modified with PC and $CoWO_4$ nanosheets, respectively. Error bars: standard deviation ($n = 3$).

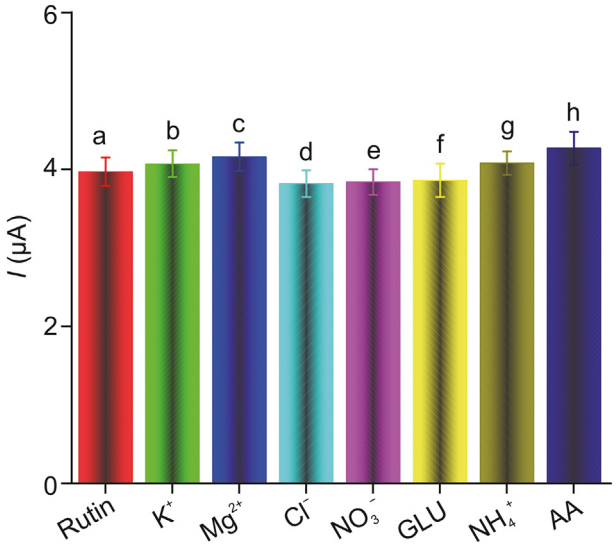

Fig. 9. DPV response of rutin samples in the presence of various interfering compounds: (a) 50 ng rutin; (b) 50 ng rutin + 1 mM K^+; (c) 50 ng rutin +1 mM Mg^{2+}; (d) 50 ng rutin +1 mM Cl^-; (e) 50 ng rutin + 1 mM NO_3^-; (f) 50 ng rutin +1 μM glucose ; (g) 50 ng rutin +1 mM NH_4^+; and (h) 50 ng rutin +1 μM ascorbic acid (AA).

Table 1
Comparison of the developed sensor in this paper with other methods for rutin detection.

Method	Electrode	Linear range (μg/mL)	Detection limit (μg/mL)	Refs.
Chemiluminescence	–	0.001–0.4	0.003	[7]
Fluorescence	–	0.061–6.1	0.012	[8]
Spectrophotometry	–	2.5–22.5	0.07	[9]
High-performance liquid chromatography	–	10–26	0.40	[10]
Capillary electrophoresis	–	0.5–50	0.01–0.24	[11]
Electrochemical	AuNPs/p-MWCNs	0.0006–0.018	0.0002	[14]
Electrochemical	RuNPs/C4A5/RGO	0.00006–0.006	0.00001	[15]
Electrochemical	$CoFe_2O_4$	0.00006–0.006	0.00002	[16]
Electrochemical	GO-Cs/GCE	0.55–54.95	0.34	[37]
Electrochemical	CB/WO_3/SPCE	0.006–46.07	0.001	[38]
Electrochemical	$NiCo_2O_4$/rGO	0.06–4.9 and 0.049–91.58	0.006	[39]
Electrochemical	C_3N_4-RGO/GCE	0.003–85.47	0.0006	[40]
Electrochemical	PC/$CoWO_4$	0.005–5	0.00045	This work

NPs: nanoparticles; p-MWCNs: p-multi-walled carbon nanotubes; rGO: reduced graphene oxide; GCE: glassy carbon electrode; CB: carbon black; SPCE: screen-printed carbon electrode; PC: porous carbon.

Table 2
Recovery results for rutin determination in commercial tablet samples ($n = 3$).

Sample	Content (ng/mL)	Added (ng/mL)	Found (ng/mL)	RSD (%)	Recovery (%)
PBS 1	0	10	10.2	3.20	102.0
PBS 2	0	100	104.5	3.10	104.5
PBS 3	0	1000	981.9	4.40	98.2
Tablet 1	10	0	9.5	4.71	95.0
Tablet 2	100	0	105.6	3.48	105.6
Tablet 3	1000	0	966.4	3.28	96.6
Human serum 1	0	0	0	0	0
Human serum 2	0	10	9.1	6.98	91.0
Human serum 3	0	100	92.4	7.71	92.4
Human serum 4	0	1000	935.6	7.23	93.6

RSD: relative standard deviation; PBS: phosphate buffered saline.

rutin was also found to depend on the pH. The results showed that the oxidation peak current reached the maximum value at pH 6.5. Meanwhile, the regression line of the oxidation peak potential was obtained as follows (Fig. 7B): The anodic peak potential (E_{pa}) = 0.7958−0.0731 pH ($R^2 = 0.9942$). Thus, a linear relationship was identified between E_{pa} and the pH value.

3.4. Analytical performance of the electrochemical sensor

The analytical performance of the sensors was estimated by the DPV method under optimal conditions, using a series of rutin concentrations ranging from 0 to 10,000 ng/mL. As shown in Fig. 8A, upon addition of rutin, the oxidation peak current at 0.25 V clearly increased, and there was a good linear relationship between the current response and the lg of the rutin concentration in the range from 5 to 5000 ng/mL. The regression equation was calculated as $I = 3.1717 \times \lg c - 1.4205$ ($R^2 = 0.9916$), where I is the value for the square-wave voltammetry current, and c is the concentration of rutin (Fig. 8B). The detection limit was low (0.45 ng/mL), and the results of rutin determination were compared with those of various other sensors in Table 1 [7–11,14–16,37–40]. As illustrated, the sensor of the PC/$CoWO_4$ modified electrode offers some advantages with a wide linearity range and a low detection limit.

3.5. Fabrication stability and reproducibility of the electrochemical sensor

The stability of the electrodes was also examined. The detection signal was frequently measured on a daily basis for 7 consecutive days (Fig. 8C), and the relative standard deviation (RSD) in the current response was found to be 3.91%. This result indicated that the modified electrode can be used in the long term. Reproducibility experiments were also performed using several different electrodes (Fig. 8D), and an RSD of 4.68% was found, indicating good reproducibility.

3.6. Selectivity of the electrochemical sensor

The selectivity of the electrochemical sensor was evaluated under the optimized experimental conditions described above. The effects of the various interfering species present in pharmaceutical rutin products and various substances (including K^+, Mg^{2+}, Cl^-, NO_3^-, glucose, NH_4^+, and ascorbic acid) were studied in the presence of rutin (50 ng/mL). Interfering compounds were found to have little effect on the detection signal of rutin (Fig. 9), demonstrating that the developed sensor has a high selectivity for rutin. This sensitivity is attributed to two main factors: 1) the high selectivity of the material adsorbed by the composite (having good adsorption capacity for hydrophobic materials), and 2) the electrochemical sensor has high selectivity as different electrically active substances have different oxidation peak potentials in DPV. This ensures high selectivity for rutin determination even in the presence of interfering species.

3.7. Analysis of rutin in real samples

To investigate the applicability of the proposed electrochemical sensor to monitor rutin in real samples, the rutin contents of medicinal tablets and human serum samples were measured by the standard addition method, and rutin (20 mg/tablet) was ground into a powder. The powdered tablet was accurately weighed and dissolved in methanol to make a stock solution, before diluting with PBS to obtain the desired concentration. DPV was carried out three times for each tablet. After adding four different concentrations of rutin to 0.5 mL samples of normal human serum, acetonitrile (1 mL) was added before incubation for 2 min followed by centrifugation (21,124 *g*, 15 min). The supernatant was dried in 50 °C nitrogen, and then PBS was added for re-determination. The results are given in Table 2. A good recovery, in the range of 91.0%–105.6%, was achieved using PC/$CoWO_4$-modified electrodes, and reliable RSD values (3.10–7.71) were obtained. The results demonstrate that the developed sensor can accurately determine the rutin content in biological samples.

4. Conclusions

In this work, an electrochemical sensor was developed based on PC and $CoWO_4$ nanosheets for the determination of rutin. Interestingly, the introduction of porous carbon as a conducting support was found to significantly improve the electrochemical performance of 3D $CoWO_4$ for rutin detection. The electrochemical sensor showed high sensitivity, specificity, repeatability, and reproducibility under the determined optimum conditions, with a wide linearity range of 5–5000 ng/mL and a detection limit of 0.45 ng/mL. The sensor was successfully applied to determine rutin in human serum samples with good recovery. The PC/$CoWO_4$-based sensor is therefore an excellent tool for electroanalysis and could be employed in the design and development of new devices.

CRediT author statement

Guangjun Feng: Validation, Conceptualization, Methodology; **Yang Yang:** Data curation, Writing - Original draft preparation; **Jiantao Zeng:** Visualization, Supervision; **Jun Zhu:** Data curation, Resources; **Jingjian Liu:** Software, Supervision; **Lun Wu:** Project administration, Formal analysis; **Zhiming Yang:** Validation; **Guanyi Yang:** Supervision; **Quanxi Mei:** Resources; **Qinhua Chen:** Data curation, Project administration; **Fengying Ran:** Software, Writing - Reviewing and Editing, Data curation.

Declaration of competing interest

The authors declare that there are no conflicts of interest.

Acknowledgments

This work was financially supported by the National Natural Science Foundation of China (Grant No.: 81872509) and the Baoan TCM Development Foundation (Grant No.: 2020KJCX-KTYJ-200), Internal Research Project of the Shenzhen Baoan Authentic TCM Therapy Hospital (Grant Nos.: BCZY2021003 and BCZY2021007), Baoan District Medical and Health Basic Research Project (Grant No.: 2020JD491), Natural Science Foundation of Hubei Province (Grant No.: 2019CFB429), Chinese Medicine Research Fund of Health Commission of Hubei Province (Grant Nos.: ZY2021M038 and ZY2021M051), the Youth Talent Project of Sinopharm Dongfeng General Hospital (Grant No.: 2021Q03), the Science and Technology Key Program of Shiyan (Grant No.: 21Y77), Baoan District Medical and Health Basic Research Project (Grant Nos.: 2021JD143, 2021JD281, and 2021JD290), Hubei Province Health and Family Planning Scientific Research Project (Grant Nos.: WJ2021M063 and WJ2021M062), and Sanming Project of Medicine in Shenzhen (Grant No.: SZZYSM202106004).

References

[1] F. Cheung, Modern TCM: Enter the clinic, Nature 480 (2011) S94–S95.
[2] S. Habtemariam, Flavonoids as inhibitors or enhancers of the cytotoxicity of tumor necrosis factor-alpha in L-929 tumor cells, J. Nat. Prod. 60 (1997) 775–778.
[3] C.Q. Hu, K. Chen, Q. Shi, et al., Anti-AIDS agents, 10. Acacetin-7-*O*-beta-D-galactopyranoside, an anti-HIV principle from *Chrysanthemum morifolium* and a structure-activity correlation with some related flavonoids, J. Nat. Prod. 57 (1994) 42–51.
[4] W. Sun, X. Wang, C. Luo, CdSe Quantum dots combined with poly(-diallyldimethylammonium chloride)-modified reduced graphene oxide for rutin determination, Chem. Lett. 47 (2018) 1438–1440.
[5] I.V. Koval Skii, I.I. Krasnyuk, O.I. Nikulina, et al., Mechanisms of rutin pharmacological action (review), Pharm. Chem. J. 48 (2014) 73–76.
[6] S. Sharma, A. Ali, J. Ali, et al., Rutin: Therapeutic potential and recent advances in drug delivery, Expert Opin. Investig. Drugs 22 (2013) 1063–1079.
[7] Z. Song, L. Wang, Chemiluminescence investigation of detection of rutin in medicine and human urine using controlled-reagent-release technology, J. Agric. Food Chem. 49 (2001) 5697–5701.
[8] B. Wang, R. Gui, H. Jin, et al., Red-emitting BSA-stabilized copper nanoclusters acted as a sensitive probe for fluorescence sensing and visual imaging detection of rutin, Talanta 178 (2018) 1006–1010.
[9] H. Xu, Y. Li, H.W. Tang, et al., Determination of rutin with UV-vis spectrophotometric and laser-induced fluorimetric detections using a non-scanning spectrometer, Anal. Lett. 43 (2010) 893–904.
[10] Y. Shen, H. Yin, B. Chen, et al., Validated reversed phase-high performance liquid chromatography-diode array detector method for the quantitation of Rutin, a natural immunostimulant for improving survival in aquaculture practice, in toonea sinensis folium, Pharmacogn. Mag. 8 (2012) 49–53.
[11] A.F. Memon, I.M. Palabiyik, A.R. Solangi, et al., Large volume sample stacking (LVSS) in capillary electrophoresis (CE) with response surface methodology (RSM) for the determination of phenolics in food samples, Anal. Lett. 15 (2019) 2853–2867.
[12] Z. Gan, Q. Chen, Y. Fu, et al., Determination of bioactive constituents in Flos Sophorae Immaturus and Cortex Fraxini by capillary electrophoresis in combination with far infrared-assisted solvent extraction, Food Chem. 130 (2012) 1122–1126.
[13] Š. Komorsky-Lovrić, I. Novak, Abrasive stripping voltammetry of myricetin and dihydromyricetin, Electrochim. Acta 98 (2013) 153–156.
[14] M.L. Yola, N. Atar, A novel voltammetric sensor based on gold nanoparticles involved in p-aminothiophenol functionalized multi-walled carbon nanotubes: Application to the simultaneous determination of quercetin and rutin, Electrochim. Acta 119 (2014) 24–31.
[15] S. Elçin, M.L. Yola, T. Eren, et al., Highly selective and sensitive voltammetric sensor based on ruthenium nanoparticle anchored calix[4]amidocrown-5 functionalized reduced graphene oxide: Simultaneous determination of quercetin, Morin and rutin in grape wine, Electroanalysis 28 (2016) 611–619.
[16] M.L. Yola, C. Göde, N. Atar, et al., Determination of rutin by $CoFe_2O_4$ nanoparticles ionic liquid nanocomposite as a voltammetric sensor, J. Mol. Liq. 246 (2017) 350–353.
[17] X.-Q. Lin, J.-B. He, Z.-G. Zha, Simultaneous determination of quercetin and rutin at a multi-wall carbon-nanotube paste electrodes by reversing differential pulse voltammetry, Sens. Actuators B Chem. 119 (2006) 608–614.
[18] R. Xing, X. Zhao, Y. Liu, et al., Low cost and reliable electrochemical sensor for rutin detection based on Au nanoparticles-loaded ZnS nanocomposites, J. Nanosci. Nanotechnol. 18 (2018) 4651–4657.
[19] S. Tursynbolat, Y. Bakytkarim, J. Huang, et al., Highly sensitive simultaneous electrochemical determination of myricetin and rutin via solid phase extraction on a ternary Pt@r-GO@MWCNTs nanocomposite, J. Pharm. Anal. 9 (2019) 358–366.
[20] J. Zhu, B. Huang, C. Zhao, et al., Benzoic acid-assisted substrate-free synthesis of ultrathin nanosheets assembled two-dimensional porous Co_3O_4 thin sheets with 3D hierarchical micro-/nano-structures and enhanced performance as battery-type materials for supercapacitors, Electrochim. Acta 313 (2019) 194–204.
[21] X. Zhao, L. Mao, Q. Cheng, et al., Recent advances in two-dimensional spinel structured Co-based materials for high performance supercapacitors: A critical review, Chem. Eng. J. 387 (2020), 124081.
[22] Y. Han, K. Choi, H. Oh, et al., Cobalt polyoxometalate-derived $CoWO_4$ oxygen-evolving catalysts for efficient electrochemical and photoelectrochemical water oxidation, J. Catal. 367 (2018) 212–220.
[23] L. Lin, W. Lei, S. Zhang, et al., Two-dimensional transition metal dichalcogenides in supercapacitors and secondary batteries, Energy Storage Mater. 19 (2019) 408–423.
[24] P. Das, Z.-S. Wu, F. Li, et al., Two-dimensional energy materials: Opportunities and perspectives, Energy Storage Mater. 22 (2019) 15–17.
[25] F. Cao, M. Zhao, Y. Yu, et al., Synthesis of two-dimensional $CoS_{1.097}$/nitrogen-doped carbon nanocomposites using metal-organic framework nanosheets as precursors for supercapacitor application, J. Am. Chem. Soc. 138 (2016) 6924–6927.
[26] B. Huang, H. Wang, S. Liang, et al., Two-dimensional porous cobalt–nickel tungstate thin sheets for high performance supercapattery, Energy Storage Mater. 32 (2020) 105–114.
[27] Q. Yun, Q. Lu, X. Zhang, et al., Three-dimensional architectures constructed from transition-metal dichalcogenide nanomaterials for electrochemical energy storage and conversion, Angew Chem. Int. Ed. Engl. 57 (2018) 626–646.
[28] S. Khaja Hussain, B.N.V. Krishna, G. Nagaraju, et al., Porous Co-MoS_2 @Cu_2MoS_4 three-dimensional nanoflowers via *in situ* sulfurization of Cu_2O nanospheres for electrochemical hybrid capacitors, Chem. Eng. J. 403 (2021), 126319.
[29] H. Xia, Q. Xu, J. Zhang, Recent progress on two-dimensional nanoflake Ensembles for energy storage applications, Nanomicro Lett. 10 (2018), 66.
[30] L. Zhao, Y. Zhang, L.-B. Huang, et al., Cascade anchoring strategy for general mass production of high-loading single-atomic metal-nitrogen catalysts, Nat. Commun. 10 (2019), 1278.
[31] S. Kaipannan, P.A. Ganesh, K. Manickavasakam, et al., Waste engine oil derived porous carbon/ZnS nanocomposite as bi-functional electrocatalyst for supercapacitor and oxygen reduction, J. Energy Storage 32 (2020), 101774.
[32] X. Xing, Y. Gui, G. Zhang, et al., $CoWO_4$ nanoparticles prepared by two methods displaying different structures and supercapacitive performances, Electrochim. Acta 157 (2015) 15–22.
[33] Y. Zhang, S. Liu, Y. Li, Electrospun graphene decorated $MnCo_2O_4$ composite nanofibers for glucose biosensing, Biosens. Bioelectron. 66 (2015) 308–315.
[34] Y. Chen, Y. Li, D. Deng, et al., Effective immobilization of Au nanoparticles on TiO_2 loaded graphene for a novel sandwich-type immunosensor, Biosens. Bioelectron. 102 (2018) 301–306.
[35] A. John, L. Benny, A.R. Cherian, et al., Electrochemical sensors using conducting polymer/noble metal nanoparticle nanocomposites for the detection of various analytes: A review, J. Nanostructure Chem. 11 (2021) 1–31.
[36] M.U. Anu Prathap, B. Kaur, R. Srivastava, Electrochemical sensor platforms based on nanostructured metal oxides, and Zeolite-based materials, Chem. Rec. 19 (2019) 883–907.
[37] M. Arvand, A. Shabani, M.S. Ardaki, A new electrochemical sensing platform based on binary composite of graphene oxide-chitosan for sensitive rutin determination, Food Anal. Methods. 10 (2017) 2332–2345.
[38] S. Kupendrian, R. Sakthivel, S.-M. Chen, et al., "Design of novel WO_3/CB nanohybrids" an affordable and efficient electrochemical sensor for the detection of multifunctional flavonoid rutin, Inorg. Chem. Front. 5 (2018) 1085–1093.
[39] S. Cui, L. Li, Y. Ding, et al., Mesoporous $NiCo_2O_4$-decorated reduced graphene oxide as a novel platform for electrochemical determination of rutin, Talanta 164 (2017) 291–299.
[40] J. Wang, B. Yang, S. Liu, et al., Enhanced photo-electrochemical response of reduced graphene oxide and C_3N_4 nanosheets for rutin detection, J. Colloid Interface Sci. 506 (2017) 329–337.